Inactivation of the endotoxic biomolecule lipid A by oxygen plasma species : a reactive molecular dynamics study

Inactivation of the endotoxic biomolecule lipid A by oxygen plasma species: a reactive molecular dynamics study

Maksudbek Yusupov[1,*], Erik C Neyts[1], Christof C Verlackt[1], Umedjon Khalilov[1], Adri C T van Duin[2] and Annemie Bogaerts[1]

[1] Department of Chemistry, Research Group PLASMANT, University of Antwerp, Universiteitsplein 1, B-2610 Wilrijk-Antwerp, Belgium

[2] Department of Mechanical and Nuclear Engineering, Penn State University, University Park, Pennsylvania 16802, United States

Keywords:

cold plasma; computer modeling; molecular dynamics; radicals; amino acids

Abstract.

Reactive molecular dynamics simulations are performed to study the interaction of reactive oxygen species, such as OH, HO_2 and H_2O_2, with the endotoxic biomolecule lipid A of the gram-negative bacterium *Escherichia coli*. It is found that the aforementioned plasma species can destroy the lipid A, which consequently results in reducing its toxic activity. All bond dissociation events are initiated by hydrogen-abstraction reactions. However, the mechanisms behind these dissociations are dependent on the impinging plasma species, i.e. a clear difference is observed in the mechanisms upon impact of HO_2 radicals and H_2O_2 molecules on one hand and OH radicals on the other hand. Our simulation results are in good agreement with experimental observations.

1. Introduction

Healthcare-associated infections (HAIs) or infections acquired in hospitals are a major public health problem, leading to significant mortality and financial losses for health systems. According to a report of the European Centre for Disease Prevention and Control (ECDC), approximately 3.2 million patients were estimated to obtain an HAI in 2011-2012 in European acute care hospitals. It was also confirmed by the ECDC that the five most frequent HAI types were respiratory tract infections, surgical site infections, urinary tract infections, bloodstream infections and gastro-intestinal infections.[1]

HAIs are partially caused by infectious agents (i.e., viruses, prions, bacteria, etc.) found on medical devices, such as endoscopes, surgical instruments and diagnostic systems. Consequently, a thorough removal of these pernicious biomolecules is needed and is achieved by either disinfection (i.e., reduction of the harmful microorganisms to a very low level) or by sterilization (i.e., removal or killing of all forms of microbial life, such as fungi, bacteria, viruses and spore forms).

Many conventional methods can be utilized for sterilization. A widely used method is an autoclave, which is mainly applied for the inactivation of bacteria and viruses. However, it is heat-based (i.e., it works with steam at high pressure) and can thus only be used for heat-resistant items; it can cause thermal destruction when used for heat-sensitive materials such as plastics, rubbers, fiber and skin. In these cases, chemical sterilants (low temperature gases or liquid solutions) may provide an alternative. For instance, heat-sensitive materials may be exposed to low temperature reactive gases, such as ethylene oxide, hydrogen peroxide and ozone, which subsequently leads to the destruction of all microorganisms, including bacterial spores.[2]

Recent experimental studies have demonstrated that low-temperature or cold atmospheric pressure plasmas (CAPPs) can also provide an attractive option for removal of hazardous biomolecules (see e.g., the review of Moisan *et al.*[3]). Moreover, due to their nontoxic

character (i.e., they can be sustained in nontoxic gases, such as argon, hydrogen or oxygen, which is relatively safe to the medical staff, as well as to the environment) and their nonthermal nature (which is ideal for heat-sensitive materials), CAPPs may possibly replace conventional sterilization methods in the near future.[4] The use of CAPPs, not only for sterilization purposes but also in other fields in biology and medicine, is attracting growing interest and is becoming one of the key topical areas of plasma research.[5-7] Experiments are also being performed on e.g., tooth bleaching[8], treatment of skin diseases[9], killing or apoptosis of cancer cells[10-14] and even tissue regeneration.[15] Therefore, the use of CAPPs for healthcare purposes led to the emergence of a new innovative field in plasma research, i.e., co-called "Plasma Medicine".[5]

CAPPs create a wide variety of plasma species, such as reactive oxygen species (ROS) (e.g., O, OH, HO_2, H_2O_2, O_3) and reactive nitrogen species (RNS) (e.g., NO, NO_2, HNO_2, ONOOH), which are most probably responsible for plasma-induced sterilization and deactivation.[16] However, the exact interaction mechanisms between the reactive species and biological samples remain elusive. In order to control the processes occurring on the surface of the biomolecules, one needs to understand the interaction mechanisms of the plasma species with biochemically relevant structures. However, this still remains a big challenge, although some fundamental investigations were already carried out by experiments,[17-20] as well as by simulations.[21-28]

In refs. [17-20], the authors investigated the antibacterial mechanisms of plasma, including separate and synergistic effects of plasma-generated ultraviolet and vacuum ultraviolet (UV/VUV) photons and particles (or radicals) at the cellular and molecular level for different kinds of biomolecules.

For example, Bartis *et al.* examined the effects of direct plasma, plasma-generated high-energy photons in UV/VUV, and radicals on lipopolisaccharide (LPS) using an inductively coupled low-pressure plasma.[18] They found that the direct plasma treatment causes rapid

etching and deactivation of LPS: for both Ar and H_2 as feed gas, the direct treatment reduces the film thickness by ~50% after about 1 min of exposure. On the other hand, plasma-generated reactive neutrals (mostly atomic O in Ar plasma and atomic H in H_2 plasma) cause a minimal etching of the films compared to direct plasma treatment, but these species deactivate the sample. Moreover, the authors showed that the radical treatment did not significantly affect the phosphorous and nitrogen content in contrast to direct and UV/VUV treatments. In both Ar and H_2 plasmas, the C–O and C=O groups slightly increased, whereas the C–C/H bonds decreased after the radical treatment of LPS. The authors concluded that the radicals play a significant role in the deactivation and modification of the LPS and lipid A films, despite negligible material removal.

Similar conclusions were made by Chung and coworkers when studying the effects of VUV radiation, oxygen and deuterium radicals on the endotoxic biomolecule lipid A (which is the toxic part of the LPS) using a vacuum beam system.[19] The authors observed a lower etching yield for radical exposure compared to VUV-induced photolysis, i.e., the bulk chemical change was dominated by VUV photolysis, whereas the radical exposures resulted in chemical etching and modification only at the surface of the lipid A films. The phosphate moieties and intact aliphatic chains, on the other hand, all decreased significantly in the case of radical exposure, even more than in the case of the VUV- treated samples. The authors also found that after radical exposure the entodoxic activity of lipid A was significantly reduced.[19]

Using an atmospheric pressure plasma jet (APPJ), Bartis *et al.* showed the importance of oxygen species in the deactivation of LPS. They concluded that as soon as O_2 gas is added to the plasma, stronger deactivation takes place, i.e., the oxygen species are required for deactivation of LPS in the APPJ.[20] Moreover, using X-ray photoelectron spectroscopy (XPS) the authors showed a decrease in the C–C/H and a slight decrease in the O–C–O/N–C=O and O–C=O bonding, while the C–O/C=O bonds increase after a treatment of LPS by 1% O_2 in Ar

APPJ containing various N_2 concentrations.[20] The authors also found that when N_2 was added to the feed gas, the ROS were reduced, which, in turn, led to a decrease in the biological deactivation.

Complementary to experimental studies, computer simulations may also provide fundamental information about the processes occurring, both in the plasma and more importantly at the surface of living cells, which is difficult or even impossible to obtain through experiments. However, until now, very limited efforts have been spent on modeling, especially with respect to the interaction of plasma with living organisms, such as bacteria.[21-28] We refer to a recent review of Neyts *et al.*, in which a current overview of modeling efforts relevant for plasma medicine, including a discussion on the use of reactive and non-reactive potentials in plasma medicine, is given.[24]

In recent years, our group already performed reactive MD simulations closely related to plasma medicine applications. Using the ReaxFF potential, we studied the interaction of ROS with peptidoglycan (PG), which is an important component of the cell wall of gram-positive bacteria. The breaking of structurally important bonds of PG (i.e. C–O, C–N and C–C bonds) by ROS was shown, which in turn probably leads to cell wall damage.[25, 26] Moreover, also the interaction of O and OH radicals with α-linolenic acid as a model system for the free fatty acids present in the upper skin layer was investigated.[27] These calculations predicted that the abstraction of hydrogen atoms from fatty acids by O and OH radicals takes place, which in turn leads to the formation of a conjugated double bond, but also to the incorporation of alcohol or aldehyde groups, thus increasing the hydrophilic character of the fatty acids and changing the general lipid composition of the skin. This is an important result, as it demonstrates the change in homeostatic function of the skin under influence of plasma radicals.

It should be mentioned that in refs. [25, 26] we carried out reactive MD simulations under 'perfect' conditions, i.e. the PG structure was not surrounded by a liquid (bio)film. In reality,

bacteria are typically coated by an aqueous layer, which can affect the behavior and stability of the plasma species. In order to investigate this effect, we performed reactive MD simulations, in which the interaction mechanisms of ROS, such as O, OH and HO_2 radicals, as well as H_2O_2 molecules, with a water layer were studied.[28] We found that OH, HO_2 and H_2O_2 can travel deep into the water layer and are hence in principle able to reach the biomolecule. Moreover, O, OH and HO_2 radicals react with water molecules through H-abstraction reactions, whereas no H-abstraction reaction takes place in the case of H_2O_2 molecules. Note, however, that other (more macroscopic liquid phase) simulations predict that the diffusion of OH in a liquid film is limited to a very superficial layer (see e.g., ref. [23]).

In the present paper, we investigate the interaction of ROS, more specifically OH and HO_2 radicals as well as H_2O_2 molecules, with the endotoxic biomolecule lipid A of the gram-negative bacterium *E. coli*. We have chosen the above mentioned ROS as they can directly interact with the biomolecule after travelling through the liquid layer.[28] Our model system lipid A is the toxic region of the LPS. LPS (or endotoxin) is the outer leaflet of the outer membrane of gram-negative bacteria. It is composed of three parts, namely the inner hydrophobic lipid A, the core oligosaccharide, and the outer O-antigen polysaccharide. The core oligosaccharide connects the outer O-antigen polysaccharide to lipid A. When the LPS is present in the bloodstream it can result in a generalized sepsis syndrome including fever, hypotension, respiratory dysfunction, and it may even lead to multiple organ failure and death.[29]

It is known that the lipid A of *E. coli* expresses the highest endotoxic activity.[30, 31] This is due to its structure, i.e., the diphosphorylated β(1-6) linked D-glucosamine disaccharide backbone carrying six aliphatic chains. Any deviation from this structure (e.g., the number and length of the fatty acid groups) decreases its toxicity. For instance, the lipid A with a monophosphoryl group is 1000-fold less active than *E. coli* lipid A.[31] Thus, our aim in this work is to study whether the ROS destroy the lipid A structure and thereby decrease its

endotoxic activity. We also present a comparison and verification of our simulation results to experimental results.[18-20]

2. Simulation setup

In an MD simulation, the trajectories of all atoms in the system are calculated by integrating the equations of motion. Forces on the atoms are derived from the ReaxFF potential.[32] ReaxFF is based on the bond order/bond distance relationship formally introduced by Abell.[33] The total system energy is the sum of several partial energy terms that include lone pairs, undercoordination, overcoordination, valence and torsion angles, conjugation as well as hydrogen bonding. Moreover, non-bonded interactions, namely Coulomb and van der Waals energy terms, are also taken into account. These interactions are calculated between every pair of atoms, such that the ReaxFF potential is able to describe covalent bonds, ionic bonds and the whole range of intermediate interactions. A more detailed description of the energy terms used in ReaxFF can be found in ref. [34]. The electronegativity equalization method [35, 36] is used to calculate charge distributions based on geometry and connectivity.

The force field required to correctly describe the specific molecular system of lipid A should contain parameters for C, H, O, N and P atoms. A ReaxFF force field containing parameters for these atoms has been used in the work of Abolfath *et al.*[37] However, this specific force field appeared not to be suitable for an accurate description of the lipid A system as it is designed to describe DNA and related molecules. To address this problem, we combined two different force fields in this investigation, i.e., the parameters for the C/H/O/N elements are obtained from,[38] which were developed by Rahaman *et al.* for the glycine/water system, whereas the P parameters are adopted from ref. [37] (see the comparison of the bond length distributions for both force fields in the supporting information). Note that the ReaxFF

parameters are optimized to obtain good general agreement with quantum mechanical calculations for reaction energies, barriers and structures (in that order of importance).

A schematic picture of the lipid A structure in *E. coli* is presented in **Figure 1**. Its chemical structure can be found in.[30, 31] It is composed of a β(1-6) linked D-glucosamine disaccharide carrying two phosphoryl groups (at positions 1 and 4') and substituted with fatty acids, ester-linked at positions 3 and 3', and amide-linked at positions 2 and 2' (see **Figure 1(b)**). These chains are then further substituted by other fatty acids to form the lipid A molecule. Hence, in the model structure of lipid A there are two phosphoryl groups (see green color in **Figure 1(b)**) connected to a disaccharide backbone (blue color in **Figure 1(b)**) carrying six aliphatic chains (red color in **Figure 1(b)**), which are made up of 12-14-carbon chains (see **Figure 1(b)**, black circles). As was mentioned above, the lipid A is the toxic part of the LPS, which is connected to a long polysaccharide chain, called an O-antigen, by a core oligosaccharide. The polysaccharide chain and core oligosaccharide serve to protect the bacteria (by keeping the structural integrity), but as we are interested in the toxic part of the LPS, and in order to perform the simulations in a computationally efficient way, we focus only on the lipid A and we substituted the other parts by methyl residues. In other words, the repeating parts of the lipid A and the part connected to the oligosaccharide (which are specified with R and R', respectively, see **Figure 1(b)**) are replaced by methyl residues (cf. **Figure 1(a)**).

In our simulations, the lipid A structure is placed in a box with dimensions 50 Å × 70 Å × 40 Å. This box size is large enough to place the incident plasma species around the structure (see below). Periodic boundary conditions are not applied to any plane as no infinite surface is needed in the simulations. However, to prevent translation and geometric deformation of the lipid A (leading to a loss of the geometric agreement with experimental lipid A found in the cell membrane[30, 31]), parts of the structure are spatially fixed during the MD simulations (see dashed circles in **Figure 1**).

Prior to the particle impacts, the lipid A structure is equilibrated at room temperature (i.e., 300 K) for 500 ps in the canonical ensemble (i.e., NVT dynamics), employing the Bussi thermostat[39] with a coupling constant of 100 fs. In all simulations, i.e., during the thermalization, as well as during the particle impact simulations, we use a time step of 0.25 fs. To obtain statistically valid results for bond-dissociation processes and to study all possible damaging mechanisms of the lipid A, we perform 100 runs for each impinging species. At the beginning of each run, 10 incident particles of a single species (e.g., ten OH radicals) are randomly positioned at a distance of at least 10 Å around the structure and from each other, to prevent initial interactions (including long distance interactions, i.e., Coulomb and van der Waals interactions) between the plasma species and the lipid A structure. The velocity directions of incident species are chosen randomly while their initial energy corresponds to room temperature. Every simulation trajectory lasts 500 ps (i.e., 2×10^6 iterations) in the canonical ensemble (i.e., NVT dynamics); we carefully checked that this time is long enough to obtain a chemically destroyed lipid A structure, at least until one critical bond in the structure is broken (see below).

3. Results and discussion

As mentioned above, the impinging plasma species in our simulations are OH, HO_2 and H_2O_2. We realize that other ROS, such as O and O_3, as well as RNS, are also known to have bactericidal effects (see e.g.,[16, 40, 41]). Moreover, O_2 and H_2O molecules can also be of interest, as they are naturally found around bacteria. However, we do not consider these species in the present work for the following three reasons. First, our investigations on the H_2O and O_2 impacts revealed that no bond-breaking events occur in the lipid A. These molecules are found to assemble around the lipid A, having only weak attractive non-bonded interactions with the structure, which was also observed in our previous studies.[25, 26] Second, there is no need to show the bond breaking mechanisms for O atoms, as we found in our

previous simulations that O radicals exhibit the same mechanisms as the OH radicals.[25, 26] To validate the latter, we have performed test runs for O atom impacts on lipid A, and we found indeed the same bond dissociation mechanisms as for the OH radicals. Furthermore, our previous simulations indicated that O atoms cannot reach the biomolecule surface, travelling through the water layer; they immediately interact with water molecules, resulting in the formation of two OH radicals.[28] Finally, O_3 and RNS are not included in the present work, as the force field used in our simulations does not accurately describe the behavior of these species. Nevertheless, the force field is under development and we hope it will be available for the above-mentioned species in the near future. In the following subsections we will show the most frequently observed bond-breaking mechanisms in our simulations.

3.1. Damage of the head group (i.e., disaccharide and phosphoryl groups) of lipid A

The most frequently occurring interaction mechanism of OH radicals with the disaccharide part is presented in **Figure 2**. After the H-abstraction reaction by the OH radical (see black dashed circle in **Figure 2**) a water molecule is formed. Subsequently, this leads to the consecutive breaking of three C–O bonds (see gray dashed lines), as well as the formation of double C=C and C=O bonds. From the 100 simulations (i.e., 100 × 10 impacts, see above), this bond-cleavage mechanism occurs 21 times. In other words, in 2.1% of the OH radical impact cases the bond-breaking mechanism shown in **Figure 2** occurs.

A similar bond-dissociation mechanism was observed in the case of the HO_2 radical impacts. H-abstraction takes place by the HO_2 radical, leading to the formation of a H_2O_2 molecule and dissociation of C–O bonds, as shown in **Figure 2**. This mechanism occurs 12 times in the case of the HO_2 radicals over 100 simulations, i.e., from 1000 HO_2 radical impacts. Hence, the mechanism shown in figure 2 happens in 1.2% of the cases.

In **Figure 3** the most frequently observed bond-breaking mechanism in the disaccharide by HO_2 radicals is depicted. After the H-abstraction from the HO_2 radical by an O atom in the

ether group of the disaccharide (see **Figure 3**, black dashed circle) an O_2 molecule is formed. As a consequence, this leads to the dissociation of two C–O bonds (see gray dashed lines), the formation of a double C=C bond and a new hydroxyl group. Note that this mechanism is observed in our simulations 28 times over the 100 runs (i.e., 1000 impacts). In other words, in 2.8 % of the 1000 HO_2 radical impacts the mechanism illustrated in **Figure 3** occurs.

Another frequently observed bond-cleavage mechanism in the disaccharide part upon impact by HO_2 radicals is presented in **Figure 4**. Again the H-abstraction reaction from the HO_2 radical takes place, now by the OH group of D-glucosamine (see black dashed circle in **Figure 4**). This leads to the cleavage of three C–O bonds; one in the ether group, one connected to the phosphoryl group and the third one by the detachment of a water molecule (see gray dashed lines in **Figure 4**). This mechanism occurs 35 times over the 100 runs (or 1000 HO_2 radical impacts). Thus, in 3.5 % of the 1000 HO_2 radical impacts the mechanism illustrated in **Figure 4** takes place.

Similar bond-cleavage mechanisms as shown in **Figures 3** and **4** are also obtained for the H_2O_2 molecules. The only difference is that the H-abstraction reaction can now take place in two ways, i.e., either directly from the H_2O_2 molecule (in 10–20% of the cases), or from a HO_2 radical, which is formed by the reaction of H_2O_2 molecules between each other. The latter is more likely to be seen (i.e., in 80–90% of the cases). Moreover, when three H_2O_2 molecules assemble around the lipid A structure, they react with each other, dissociating into HO_2 radicals and water molecules. Subsequently, one of the HO_2 radicals can react with the lipid A structure, causing the breaking of the bonds as described in **Figures 3** and **4**. A similar dissociation mechanism of the H_2O_2 molecule was observed in our previous work.[26]

In the case of the H_2O_2 molecules the mechanisms presented in **Figures 3** and **4** occur 12 and 25 times, respectively, over the 100 simulations, i.e., from the 1000 H_2O_2 molecule impacts. In other words, in 1.2% and 2.5% of the cases, the above mentioned bond-breaking mechanisms occur upon H_2O_2 impacts.

In summary, it is clear that the OH, HO_2 and H_2O_2 plasma species can destroy the disaccharide part, leading to the dissociation of C–O bonds and the detachment of the phosphate groups, as well as the formation of water and oxygen molecules. This, in turn, leads to a decrease in O–C–O groups (see **Figures 2** and **4**) and the formation of new C=C and C=O bonds, and therefore also to a decrease in the total number of C–C and C–H bonds. Note that the above mechanisms typically occurred in a few % of the impacts, which means that these ROS are quite effective in breaking C–O bonds in the disaccharide part of lipid A, and in detaching the phosphoryl groups.

3.2. Detachment of the aliphatic chains in lipid A

The most frequently occurring interaction mechanism of OH radicals with the aliphatic chain is presented in **Figure 5**. A H atom positioned close to the ester is abstracted (see black dashed circles). This leads to the formation of a double C=C bond and the dissociation of a C–O bond in the ester, i.e., detachment of an aliphatic chain. A similar C–O bond breaking mechanism can occur from the ester of the aliphatic chain with 12 carbons (see **Figure 1(b)**). This mechanism is observed in our simulations 17 times over the 100 runs, i.e., the detachment of the aliphatic chains occurs in 1.7% of the cases of 1000 OH radical impacts. Desorption of the aliphatic chains is only seen in a limited number of cases after impact of HO_2 and H_2O_2.

Thus, we can conclude that OH radicals can react with the H atom, which is closely positioned to the ester, and can lead to the detachment of the aliphatic chains, either as $C_{14}H_{27}O_2^*$ or $C_{12}H_{23}O_2^*$. This results in a decrease of the total number of ester (O–C=O) groups. On the other hand, detachment of the aliphatic chains after HO_2 or H_2O_2 impacts is almost negligible.

3.3. General discussion and comparison with experiments

Table 1 presents the number of C–O and C–H bonds broken upon impact of OH, HO_2 and H_2O_2 species, per impacting particle. We should mention that in our simulations ten impinging particles (e.g., ten OH radicals) hit the surface (almost) simultaneously, so more than one bond-breaking event can occur within one simulation (i.e., within the total simulation time of 500 ps). To take this into account we divide the total number of broken bonds per simulation by ten. Thus, in the following we report all bond breaking events per particle impact. Note that in total there are 29 C–O bonds and 177 C–H bonds in the structure. Hence, it looks as if the chance of bond breaking is not very large (around 1% or lower), but the cleavage of even a single C–O bond could possibly destroy the structure and therefore reduce already the toxicity of lipid A, and moreover, in reality several plasma species can impact at the same time. Indeed, if any of the aforementioned mechanisms (see **Figures 2–5**) take place, this will most likely eventually result in a decrease of the toxicity of lipid A. For instance, as mentioned above, the lipid A with a monophosphoryl group (see mechanisms shown in **Figures 2–4**) is 1000-fold less active than *E. coli* lipid A.[31] Moreover, the number of aliphatic chains has a direct effect on lipid A's toxicity; a structure with six fatty acid groups expresses the optimal endotoxic activity. The length of the fatty acid chains is also important for the toxicity as C_{12}, $C_{12}OH$, C_{14}, and $C_{14}OH$ fatty acids are those found in the most toxic lipid A structures.[42]

It is obvious from **Table 1** that the HO_2 radicals are more effective in breaking C–O bonds, followed by the H_2O_2 molecules, while the OH radicals are less effective. This was also clear from the discussion above (**section 3.1**), because more mechanisms for C–O bond breaking exist in the disaccharide part upon HO_2 impact than upon OH impact. On the other hand, in the case of the C–H bond breakings, the OH radicals are clearly more effective, followed by HO_2 and H_2O_2. This is again logical, as the OH radicals always start with H-abstraction from

the structure, whereas in the case of HO_2 and H_2O_2 impact, the mechanism starts with H-abstraction from the impacting species.

It should be mentioned that in our simulations we have not observed any C–C and P–O bond breaking events upon impact of OH, HO_2 and H_2O_2 species. Moreover, the cleavage of C–N bonds was found to be negligible compared to C–O bond breaking, i.e., the dissociation of C–N bonds occurs only few times for the cases of HO_2 and H_2O_2 impact, whereas no C–N bonds are broken in the case of OH radicals.

The percentages of the bond-breaking processes/mechanisms, which are shown in **Figures 2–5**, are given in each figure caption and summarized here in **Table 2**.

It is worth noting that in each of these mechanisms at least one (and maximum three) C–O bond is dissociated (see **Figures 2–5**). It should also be mentioned that in this work we have shown most frequently occurring bond-cleavage mechanisms.

Finally, we have compared our simulation results with experimental observations,[18-20] and in general, good qualitative agreement is reached. Indeed, Bartis *et al.* reported that reactive oxygen species are required for deactivation of LPS in the APPJ.[20] The authors have also shown a decrease in C–C/H and a slight decrease in the O–C–O/N-C=O and O–C=O bonding, by means of XPS, while the C–O/C=O groups increased when treating LPS with ROS.[20] We can assume that the decrease in C–C and C–H groups is probably due to the following. All bond-breaking mechanisms upon impact of OH radicals are initiated by the dissociation of C–H bonds (i.e., the H-abstraction reactions; see **Figures 2** and **5** above). This leads, among others, to the formation of double C=C bonds. Hence, the total number of C–C and C–H bonds will decrease (which causes a decrease in the C–C and C–H signals in the XPS spectra), despite the fact that we do not see the direct breaking of C–C bonds (at least for OH, HO_2 and H_2O_2 impacts). On the other hand, we do see the breaking of O–C–O bonds (see **Figures 2** and **4**), as well as the detachment of aliphatic chains, i.e., breaking of O–C=O groups (see **Figure 5**), in agreement with the XPS measurements.[20] Moreover, this bond

breaking leads to the formation of double C=O bonds (i.e., increase in C=O groups, which is also observed in ref. [20]). The increase in C-O groups in our simulations is observed only for the OH radical impacts (i.e., not for the HO_2 and H_2O_2 impacts) and it occurs solely in the aliphatic chains. This C–O increase is due to the creation of new hydroxyl groups in the aliphatic chains. The mechanism is as follows. One of the OH radicals abstracts the H atom from a $–CH_2–$ group of the aliphatic chain (see **Figure 1**), leading to the formation of a –HC•– radical. Subsequently, another OH radical attaches to the –HC•– radical, resulting in the formation of a new hydroxyl group (i.e., a new C–O bond). This mechanism is observed in our simulation 9 times out of 1000 OH radical impacts (i.e., in 0.9% of the cases). We also observed a similar mechanism in our test simulations with O radicals. O atom can abstract the H atom from the aliphatic chain and immediately attach to it, leading to the formation of new hydroxyl group. Moreover, O atoms can also break the C–C bonds in the aliphatic chains and form carbonyl groups (i.e., new C=O bonds, see the supporting information).

It needs to be stressed here that the experiments were performed on LPS, where interactions between the reactive species and the O-antigen and/or the core oligosaccharide are also possible. This can result in the formation of new C–O/C=O groups, as well as the dissociation of C–C bonds.

We also compared our results with the experimental work by Chung *et al.*,[19] as they studied the effects of VUV radiation, oxygen and deuterium radicals on the endotoxic biomolecule lipid A. These authors found that the phosphate moieties and intact aliphatic chains all decreased significantly in the case of radical exposures (mainly due to O radicals, see ref. [19]) even more than that of the VUV-treated samples. This was also observed in our simulations, especially upon impact of the OH radicals, which have the same reaction mechanisms as the O radicals.

Finally, we observed no bond breaking events in the phosphoryl groups (i.e., no P–O bonds were broken) as well as negligible breaking of the C–N bonds, which is consistent with the

observations of Bartis *et al.*, who also reported that the radical treatment did not significantly affect the phosphorous and nitrogen content, in contrast to direct and UV/VUV treatments of LPS.[18]

4. Conclusions

We investigated the interaction of ROS, more specifically OH and HO_2 radicals as well as H_2O_2 molecules, with the lipid A structure on the atomic level by means of reactive MD simulations. We found that these plasma species can destroy the lipid A structure, which leads to a decrease of its toxicity. Destruction of different parts of the lipid A structure, namely the hydrophilic head (i.e., the disaccharide and phosphoryl groups) and the aliphatic chains, were thoroughly investigated, for the impacts of OH and HO_2 radicals as well as H_2O_2 molecules. It was found that the interaction mechanisms are in all cases initiated by H-abstraction reactions, which mainly take place from the impinging particle itself in the cases of HO_2 and H_2O_2 by the lipid A structure, whereas in the case of OH radicals, the radical abstracts the H atom from the lipid A structure. Note, however, that other (macroscopic) simulations indicate that the diffusion of OH radicals in a liquid film might be limited to a very superficial layer, as they can recombine into H_2O_2 (see e.g., ref. [23]). However, while it is indeed true that the free energy of solvation for OH is more negative in the air/water interface (-24 kJ/mol), it is also negative in the water bulk (-18 kJ/mol).[43] Thus, since the plasma will continuously generate OH, the reservoir function of the superficial layer will be quickly saturated, and OH is likely to also diffuse into the bulk liquid, where it attains a concentration enhanced by a factor of 1100 relative to the gas phase. Moreover, it is known that under some conditions, the plasma jet can blow away (part of) the liquid film,[44] rendering the inclusion of OH even more justified.

The obtained results are in good qualitative agreement with experimental observations.[18-20] Therefore, our simulations can be useful for improving our understanding about the

destruction mechanisms of lipid A molecules, and hence, to obtain a better insight in the antibacterial properties of plasmas.

Acknowledgements:

This work was financially supported by the Fund for Scientific Research Flanders (FWO). The work was carried out in part using the Turing HPC infrastructure of the CalcUA core facility of the Universiteit Antwerpen, a division of the Flemish Supercomputer Center VSC, funded by the Hercules Foundation, the Flemish Government (department EWI) and the Universiteit Antwerpen. The authors thank S. Aernouts for the interesting discussions.

References:

[1] European Centre for Disease Prevention and Control. Point prevalence survey of healthcare associated infections and antimicrobial use in European acute care hospitals. Stockholm: ECDC; **2013**

[2] W. A. Rutala, D. J. Weber, *Clin. Infect. Dis.* **2004**, *39*, 702.

[3] M. Moisan, J. Barbeau, S. Moreau, J. Pelletier, M. Tabrizian, L. H. Yahia, *Int. J. Pharm.* **2001**, *226*, 1.

[4] M. Laroussi, *Plasma Process. Polym.* **2005**, *2*, 391.

[5] M. G. Kong, G. Kroesen, G. Morfill, T. Nosenko, T. Shimizu, J. van Dijk, J. L. Zimmermann, *New J. Phys.* **2009**, *11*, 115012.

[6] K. Ostrikov, E. C. Neyts, M. Meyyappan, *Adv. Phys.* **2013**, *62*, 113.

[7] M. Yousfi, N. Merbahi, A. Pathak, O. Eichwald, *Fundam. Clin. Pharmacol.* **2013**, *27*, 1.

[8] H. W. Lee, G. J. Kim, J. M. Kim, J. K. Park, J. K. Lee, G. C. Kim, *J. Endod.* **2009**, *35*, 587.

[9] A. B. Shekhter, V. A. Serezhenkov, T. G. Rudenko, A. V. Pekshev, A. F. Vanin, *Nitric Oxide* **2005**, *12*, 210.

[10] H. M. Joh, S. J. Kim, T. H. Chung, S. H. Leem, *Appl. Phys. Lett.* **2012**, *101*, 053703.

[11] J. Huang, H. Li, W. Chen, G-H. Lv, X-Q. Wang, G-P. Zhang, K. Ostrikov, P-Y. Wang, S-Z. Yang, *Appl. Phys. Lett.* **2011**, *99*, 253701.

[12] N. Barekzi, M. Laroussi, *J. Phys. D: Appl. Phys.* **2012**, *45*, 422002.

[13] K. K. Nagendra, H. K. Yong, G. H. Yong, H. C. Eun, *Appl. Phys.* **2012**, *13*, 176.

[14] S. Zhao, Z. Xiong, X. Mao, D. Meng, Q. Lei, Y. Li, P. Deng, M. Chen, M. Tu, X. Lu, G. Yang, G. He, *PLoS ONE* 2012, **8**, e73665.

[15] G. Fridman, G. Friedman, A. Gutsol, A. B. Shekhter, V. N. Vasilets, A. Fridman, *Plasma Process. Polym.* **2008**, *5*, 503.

[16] D. B. Graves, *J. Phys. D: Appl. Phys.* **2012**, *45*, 263001.

[17] J-W. Lackmann, S. Schneider, E. Edengeiser, F. Jarzina, S. Brinckmann, E. Steinborn, M. Havenith, J. Benedikt, J. E. Bandow, *J. R. Soc. Interface* **2013**, *10*, 20130591.

[18] E. A. J. Bartis, C. Barrett, T-Y. Chung, N. Ning, J-W. Chu, D. B. Graves, J. Seog, G. S. Oehrlein, *J. Phys. D: Appl. Phys.* **2014**, *47*, 045202.

[19] T-Y. Chung, N. Ning, J-W. Chu, D. B. Graves, E. Bartis, J. Seog, G. S. Oehrlein, *Plasma Process. Polym.* **2013**, *10*, 167.

[20] E. A. J. Bartis, D. B. Graves, J. Seog, G. S. Oehrlein, *J. Phys. D: Appl. Phys.* **2013**, *46*, 312002.

[21] N. Y. Babaeva, N. Ning, D. B. Graves, M. J. Kushner, *J. Phys. D: Appl. Phys.* **2012**, *45*, 115203.

[22] R. M. Cordeiro, *Biochim. Biophys. Acta* **2014**, *1838*, 438.

[23] W. Tian, M. J. Kushner, *J. Phys. D: Appl. Phys.* **2014**, *47*, 165201.

[24] E. C. Neyts, M. Yusupov, C. C. Verlackt, A. Bogaerts, *J. Phys. D: Appl. Phys.* **2014**, *47*, 293001.

[25] M. Yusupov, E. C. Neyts, U. Khalilov, R. Snoeckx, A. C. T. van Duin, A. Bogaerts, *New J. Phys.* **2012**, *14*, 093043.

[26] M. Yusupov, A. Bogaerts, S. Huygh, R. Snoeckx, A. C. T. van Duin, E. C. Neyts, *J. Phys. Chem. C* **2013**, *117*, 5993.

[27] J. Van der Paal, S. Aernouts, A. C. T. van Duin, E. C. Neyts, A. Bogaerts, *J. Phys. D: Appl. Phys.* **2013**, *46*, 395201.

[28] M. Yusupov, E. C. Neyts, P. Simon, G. Berdiyorov, R. Snoeckx, A. C. T. van Duin, A. Bogaerts, *J. Phys. D: Appl. Phys.* **2014**, *47*, 025205.

[29] J. Cohen, *Nature* **2002**, *420*, 885.

[30] M. Caroff, D. Karibian, *Carbohydr. Res.* **2003**, *338*, 2431.

[31] C. Erridge, E. Bennett-Guerrero, I. R. Poxton, *Microbes Infect.* **2002**, *4*, 837.

[32] A. C. T. van Duin, S. Dasgupta, F. Lorant, W. A. Goddard III, *J. Phys. Chem. A* **2001**, *105*, 9396.

[33] G. C. Abell, *Phys. Rev. B* **1985**, *31*, 6184.

[34] K. Chenoweth, A. C. T. van Duin, W. A. Goddard III, *J. Phys. Chem. A* **2008**, *112*, 1040.

[35] W. J. Mortier, S. K. Ghosh, S. Shankar, *J. Am. Chem. Soc.* **1986**, *108*, 4315.

[36] G. O. A. Janssens, B. G. Baekelandt, W. J. Mortier, R. A. Schoonheydt, *J. Phys. Chem.* **1995**, *99*, 3251.

[37] R. M. Abolfath, A. C. T. van Duin, T. Brabec, *J. Phys. Chem. A* **2011**, *115*, 11045.

[38] O. Rahaman, A. C. T. van Duin, W. A. Goddard III, D. J. Doren, *J. Phys. Chem. B* **2011**, *115*, 249.

[39] G. Bussi, D. Donadio, M. Parrinello, *J. Chem. Phys.* **2007**, *126*, 014101.

[40] A. Mahfoudh, F. Poncin-Epaillard, M. Moisan, J. Barbeau, *Surface science* **2010**, *604*, 1487.

[41] M. J. Pavlovich, H-W, Chang, Y. Sakiyama, D. S. Clark, D. B. Graves, *J. Phys. D: Appl. Phys.* **2013**, *46*, 145202.

[42] U. Zahringer, Y. A. Knirel, B. Lindner, J. H. Helbig, A. Sonesson, R. Marre, E. T. Rietschel, *Prog. Clin. Biol. Res.* **1995**, *392*, 113.

[43] R. Vacha, P. Slavicek, M. Mucha, B. J. Finlayson-Pitts, P. Jungwirth, *J. Phys. Chem. A* **2004**, *108*, 11573.

[44] T. K. Madhuri, D. Papatheodorou, A. Tailor, C. Sutton, S. Butler-Manuel *Gynecol. Surg.* **2010**, *7*, 423.

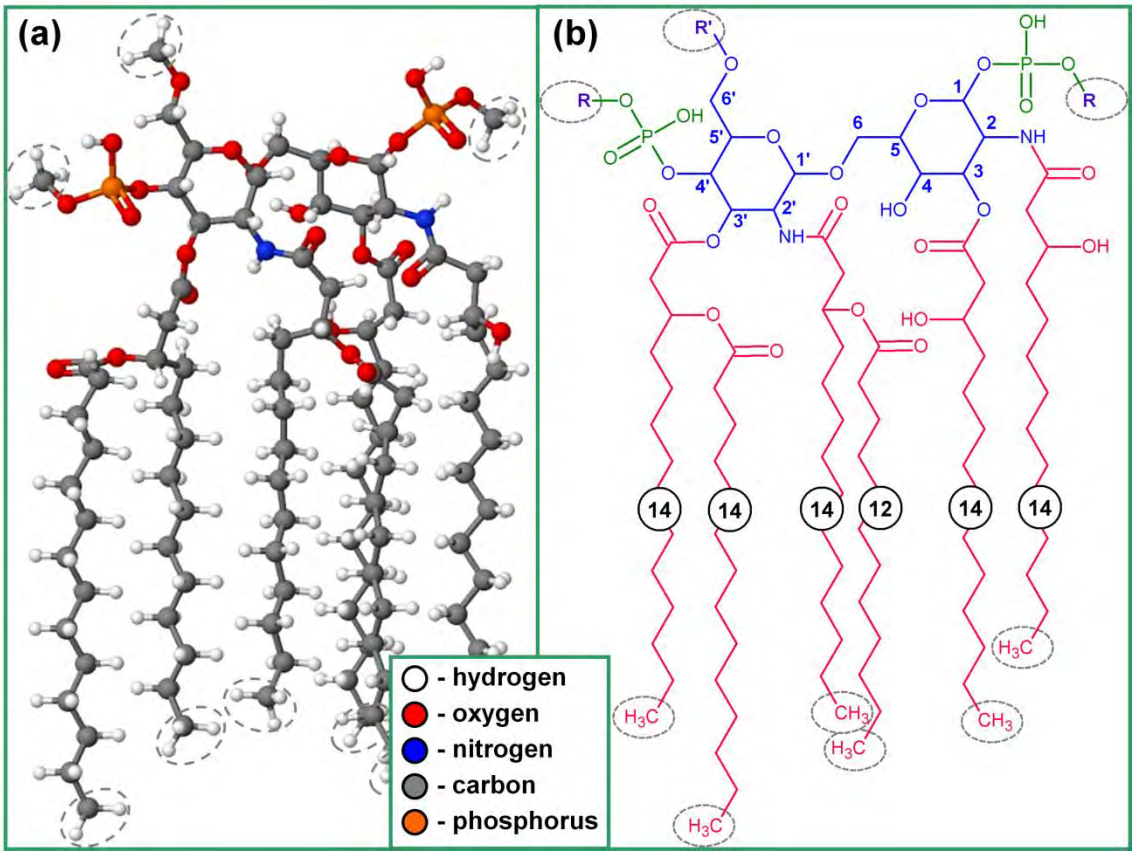

Figure 1. Schematic representation of the lipid A structure (a), and its chemical structure (b).The phosphoryl part, disaccharide backbone and aliphatic chains are indicated in (b) by green, blue and red colors, respectively. These colors also apply to the other figures below. The repeating parts of the lipid A, as well as the part connected to the oligosaccharide, are designated by R and R', respectively, which are substituted by methyl residues (cf. (a)). The number of carbons in the aliphatic chains is indicated in black circles. The fixed H atoms in all methyl residues are indicated in grey dashed circles (see (a) and (b)).

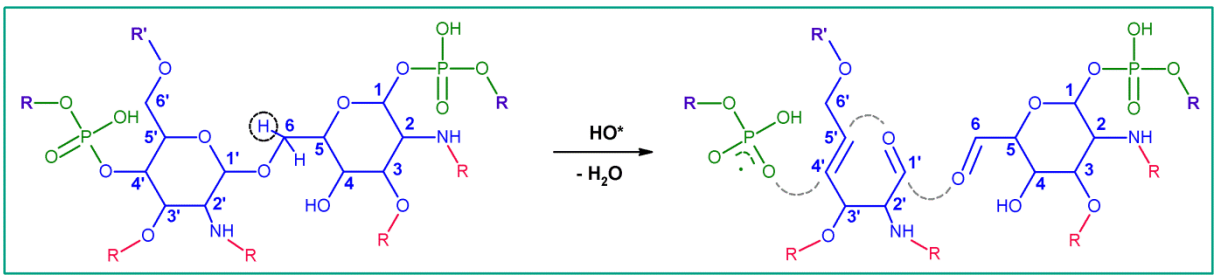

Figure 2. Breaking mechanism of three C–O bonds in the disaccharide part (see blue color and cf. Figure 1(b)) upon impact of an OH radical. The OH radical abstracts an H atom (see black dashed circle) leading to the formation of a water molecule. This subsequently results in the cleavage of three C–O bonds (see gray dashed lines) and the formation of two double C=O bonds and one double C=C bond. The aliphatic chains are substituted in this figure with R (see red color and cf. Figure 1(b)), for the sake of clarity. This mechanism occurred in 2.1% of the OH radical impact cases (and in 1.2% of the HO_2 impact cases).

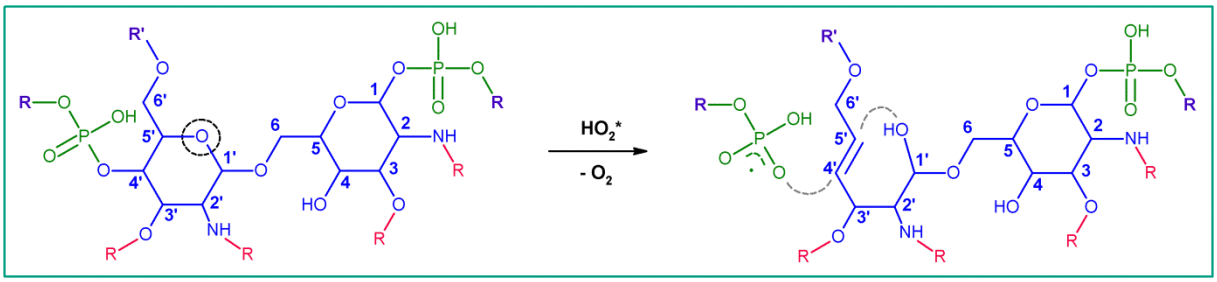

Figure 3. Breaking mechanism of two C–O bonds in the disaccharide part (see blue color and cf. Figure 1(b)) upon impact of a HO_2 radical. The 1′-5′ ether O atom (see black dashed circle) abstracts the H atom from the HO_2 radical, leaving an O_2 molecule. Subsequently, this leads to the breaking of two C–O bonds (see gray dashed lines) and the formation of a double C=C bond and a new OH group. The aliphatic chains are substituted in this figure with R (see red color and cf. Figure 1(b)), for the sake of clarity. This mechanism occurred in 2.8% of the HO_2 impact cases (and in 1.2% of the H_2O_2 impact cases).

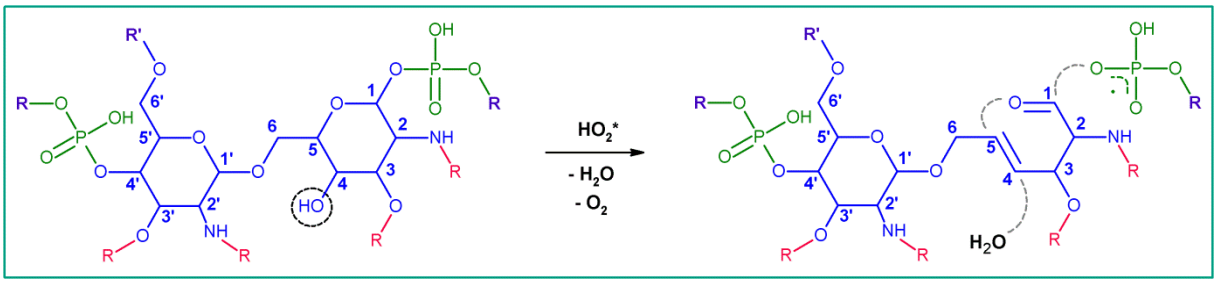

Figure 4. Breaking mechanism of three C–O bonds in the disaccharide part (see blue color and cf. Figure 1(b)) upon impact of a HO_2 radical. The OH residue of D-glucosamine connected to the carbon atom at position 4 (see black dashed circle) abstracts the H atom from the HO_2 radical, forming an O_2 molecule. Subsequently, this leads to the breaking of three C–O bonds (see gray dashed lines). Note that one of the C–O bonds is broken due to the detachment of a water molecule. The aliphatic chains are substituted in this figure with R (see red color and cf. Figure 1(b)), for the sake of clarity. This mechanism occurred in 3.5% of the HO_2 impact cases (and in 2.5% of the H_2O_2 impact cases).

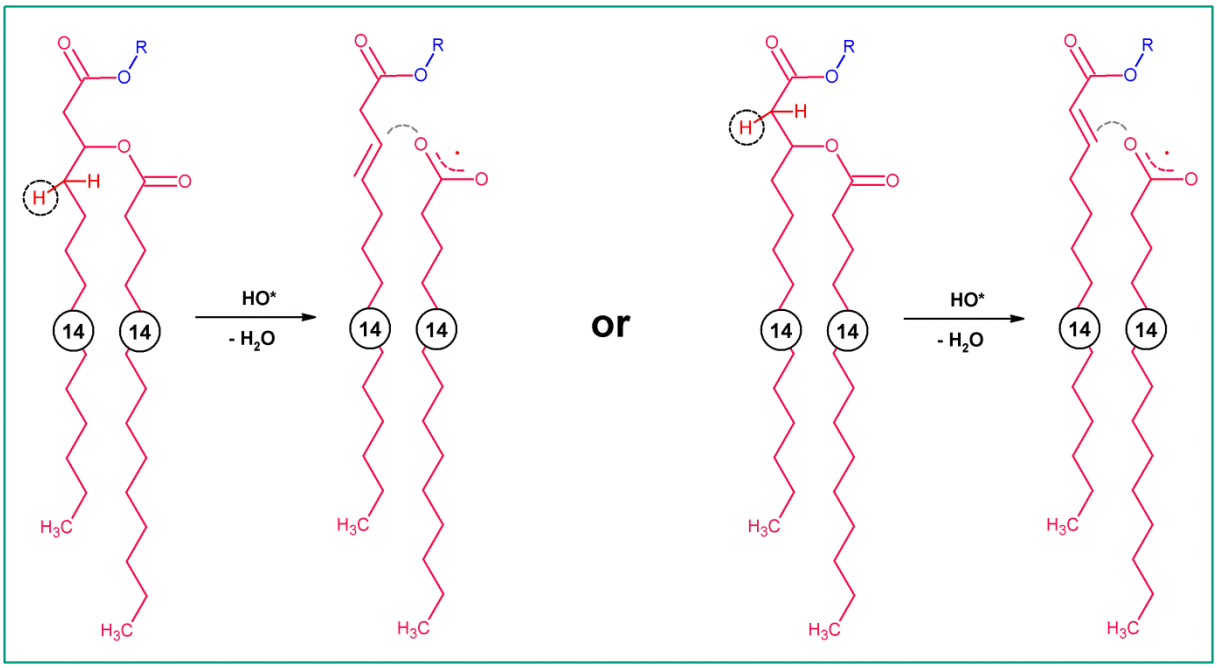

Figure 5. C-O bond breaking mechanism in the aliphatic chain (see red color and cf. Figure 1(b)) upon impact of an OH radical. The OH radical abstracts one of the H atoms (see black dashed circles), which are close to the ester group, and a water molecule is formed. This, in turn, leads to the formation of a double C=C bond, as well as the cleavage of a C–O bond (see gray dashed lines), hence detachment of an aliphatic chain. The disaccharide is substituted in this figure with R (see blue color and cf. Figure 1(b)), for the sake of clarity. This mechanism occurred in 1.7% of the OH radical impact cases, but was almost negligible in the case of the HO_2 and H_2O_2 impacts.

Table 1. Average number of dissociated C–O and C–H bonds upon impact of OH, HO_2 and H_2O_2 plasma species. The values are calculated per impacting particle for a simulation time of 500 ps, and are averaged over 100 independent simulations (i.e., 1000 impacts in total).

incident plasma species	**number of broken C–O bonds**	**number of broken C–H bonds**
OH	0.16	0.55
HO_2	0.38	0.1
H_2O_2	0.25	0.02

Table 2. Percentages of the bond-breaking mechanisms shown in Figures 2–5 (see above). Note that the values are calculated for a simulation time of 500 ps.

bond-breaking mechanism	**incident plasma particle**	**occurrence [%]**
Figure 2	OH	2.1
	HO_2	1.2
	H_2O_2	0
Figure 3	OH	0
	HO_2	2.8
	H_2O_2	1.2
Figure 4	OH	0
	HO_2	3.5
	H_2O_2	2.5
Figure 5	OH	1.7
	HO_2	negligible
	H_2O_2	negligible